

Numerical Studies on the Magnetism of Fe-Ni-Mn Alloys in the Invar Region *

A. PAINTNER, F. SÜSS and U. KREY

Institut für Physik II der Universität Regensburg,
Universitätsstr. 31, D-93040 F.R.G.

December 11, 2017

Abstract

By means of self-consistent semi-empirical LCAO calculations we study the itinerant magnetism of $(\text{Fe}_{0.65}\text{Ni}_{0.35})_{1-y}\text{Mn}_y$ alloys for y between 0 and 0.22 at $T = 0$ K, neglecting only the transverse spin components. We find that the magnetic behaviour is quite complicated on a local scale. In addition to ferromagnetic behaviour, also metastable spin-glass-like configurations are found. In the same approach, using a direct numerical calculation by the Kubo-Formalism without any fit parameters, we also calculate the electrical conductance in the magnetic state and find that the y -dependence observed in the experiments is well reproduced by our calculations, except of an overall factor of ≈ 5 , by which our resistivities are too large.

1 Introduction

In two recent papers, [1, 2], we have reported progress in the calculation of the itinerant magnetism of ordered or disordered metallic alloys in a self-consistent semi-empirical LCAO approach (LCAO= "Linear Combination of Atomic Orbitals"). In the first of those papers, [1], fcc iron and particularly disordered fcc $\text{Fe}_{1-x}\text{Ni}_x$ alloys have been treated, with particular emphasis on the so-called Invar region around $x = 0.35$,

*based on the Diploma thesis of A. Paintner, Regensburg 1994

where the local Fe moments respond quite sensitively on changes of the local neighbourhood and on the local volume. In fact, the Invar behaviour is essentially a consequence of strong magneto-volume effects (see Wassermann, [3], for a review), which happens both in face-centered and also in amorphous Fe, see [1] and [4], respectively.

In the second paper, [2], we concentrated on elemental Mn and various Mn alloys with Ni or Fe, respectively. Here it turned out that the magnetism of Mn is very complicated, e.g. α -Mn has a primitive cubic elementary cell with 58 atoms and a very complicated antiferromagnetic spin configuration. This spin configuration is not even exactly known, but seems to be non-collinear with at least eight non-equivalent magnetic sites in the elementary cell, where not only the Mn moment directions, but also the magnitudes of the moments are strongly different for these sites (see [2] for details). However, in spite of the difficulties, we finally obtained in [2] a consistent description of the parameters involved in our semi-empirical model. Here we used 9 orbitals per atom, namely five 3d-, three 4p- and one 4s-orbitals, and parametrized the hopping elements appearing in the Hamiltonian according to a Slater-Koster approach with Two-Center-Integrals up to third-nearest neighbours as given in the book of Papaconstantopoulos, [5]. Furthermore, in our semi-empirical LCAO approach the atomic charges and moments are obtained selfconsistently from a single intra-d-orbital Hubbard integral U , see [1, 2, 4]. That is, the mechanism leading to the itinerant magnetism is the interplay of Coulomb interaction and Pauli principle, according to which only two electrons with different spins can occupy the same orbital, but if they do, this costs an additional Coulomb repulsion U , so that energy can be gained by having different occupation numbers in the up- and down spin states, respectively.

At the end of paper [2], we finally also obtained consistency of the band shift parameters for the different kinds of atoms in binary alloys of Mn, Ni and Fe, respectively.

Thus we are now able to treat also the disordered ternary alloy $(\text{Fe}_{1-x}\text{Ni}_x)_{1-y}\text{Mn}_y$. Here we concentrate on the case $x = 0.35$, where without Mn one is in the above-mentioned Invar region, and where according to the experimentalists, with increasing Mn concentration y a transition to spin glass behaviour should happen (see [6, 7, 8, 9]). The problem of this transition is of special concern to us in this paper.

With our LCAO-formalism, we have also been able to calculate directly the resistivity of the alloys in the magnetic state, which has been measured by the same experimental group, [10].

Our paper is organized as follows: In chapter 2, we describe our formalism and details of the computation. In chapter 3, respectively, the results for the magnetic behaviour and for the resistivity are presented, and finally in chapter 4, we give our conclusion and discuss remaining open questions.

2 Formalism

Our alloys are modelled by 108 atoms, arranged on the sites of an fcc cube with periodic boundary conditions. The occupation of the sites with Fe, Ni and Mn atoms is performed randomly according to the formula $(\text{Fe}_{1-x}\text{Ni}_x)_{1-y}\text{Mn}_y$. For every pair of concentrations x and y considered in the results below, typically ten different random samples have been generated, from which averages have been gained. Concerning the lattice constants, we took the results presented on p. 91 of [6], according to which the y -dependence of the lattice constant a can roughly be described by a parabola passing through $a=3.59 \text{ \AA}$ at $y = 0$ and $y = 0.19$, with the minimum value of $a = 3.584 \text{ \AA}$ at $y = 0.095$ in-between.

The quantum-mechanical self-consistency equations, which have to be solved in our LCAO approximation, are

$$\sum_{m,\beta} H_{l,m}^{\alpha,\beta} c_{m,\beta,\sigma}^{(\nu)} + U_{l,\alpha} \cdot (n_{l,\alpha,-\sigma} - n_{l,\alpha}^{(para)} - \sigma \cdot \Delta_l) \cdot c_{l,\alpha,\sigma}^{(\nu)} = \epsilon_{\sigma}^{(\nu)} c_{l,\alpha,\sigma}^{(\nu)}. \quad (1)$$

Here l and m count the 108 sites, α and β the 9 orbitals per site, and $\sigma = \pm 1$ the two possible orientations of the spin; for every spin direction, the index ν counts the 9×108 possible orthonormal single-particle eigenvectors $\vec{c}_{\sigma}^{(\nu)}$ with real components $c_{l,\alpha,\sigma}^{(\nu)}$ and the corresponding single-particle energies $\epsilon_{\sigma}^{(\nu)}$. The parameter $U_{l,\alpha}$ is the above-mentioned Hubbard-type intra-orbital Coulomb integral (see below), while $n_{l,\alpha,\sigma}$ and $n_{l,\alpha}^{(para)}$ are the expectation values of the occupation numbers in the magnetic and paramagnetic state, respectively, and determined by the self-consistency equations

$$n_{l,\alpha,\sigma} = \sum_{\nu=1}^{\nu_f(\sigma)} |c_{l,\alpha,\sigma}^{(\nu)}|^2. \quad (2)$$

In eqn. (2), the sum $\nu = 1, \dots, \nu_f(\sigma)$ is over the occupied single-particle energies of the given spin-direction. In the present disordered magnetic system, these states are non-degenerate.

Of course it should be mentioned that this treatment of the Hubbard interaction corresponds to a mean-field approximation, so that in the calculation of the total energy one would have to subtract the well-known double counting correction terms from the sum of the single particle energies (see e.g. [2, 1]); however, as already mentioned above, the energies calculated from our approach are in any case not very reliable.

Finally, there appear parameters Δ_l in eqn. (1), which play the role of effective fields serving for the initialization of the magnetic state, if one starts from a paramagnetic state. These initializing fields are switched off after the first few iterations; their position dependence becomes an important point, when one wants to generate spin glass configurations (see below).

Concerning the values of $U_{l,\alpha}$, we assume as usual that they are different from 0 only for d -states and actually depend only on the kind of atom considered, namely $U_{l,\alpha} = 5.3$ eV for Fe and Ni, see [1], and 2.9 eV for Mn, see [2].

The $H_{l,m}^{\alpha,\beta}$ -matrix in eqn. (1) describes the LCAO Hamiltonian for the *paramagnetic* system. Here, the elements with $l = m$, but $\alpha \neq \beta$, vanish, while for the terms with $\alpha = \beta$, i. e. the self-energies, we use the numbers given in the book of Papaconstantopoulos, [5] p. 289 ff. And as already mentioned in [2], although the Fe values are taken from bcc Fe, they work even for fcc alloys of Fe, Ni and/or Mn, if one introduces additional self-energy -shifts $d_{Fe \rightarrow Mn} = +0.9$ eV and $d_{Fe \rightarrow Ni} = +0.95$ eV for the $H_l^{\alpha\alpha}$ -levels of Mn resp. Ni relative to the Fe levels. Of course, finally in the magnetic state the $n_{l,\alpha,\sigma}$ are in any case self-consistently determined through the U -terms in eqn. (1).

Concerning the hopping matrix elements $H_{l,m}^{\alpha,\beta}$, i.e. with $l \neq m$, we have again relied on the parametrization with two-center integrals and orthonormal orbitals in [5], and again, as in [1, 2], we take into account the fact that the distances between the sites in our alloys are different

from those in [5] by modifying the two-center integrals $I_{\alpha,\beta;\gamma}$ (e.g. with $\gamma = \sigma, \pi$ or δ) according to the *ansatz*

$$I_{\alpha,\beta;\gamma}(r) = \eta_{\alpha,\beta;\gamma} \cdot r^{-k}. \quad (3)$$

Here $k = 5$ for $(\alpha, \beta) = (d, d)$; $k = 7/2$ for $(\alpha, \beta) = (p, d)$ or (s, d) , and $k = 2$ for $(\alpha, \beta) = (s, s)$, (s, p) or (p, p) ; see Harrison [11]. The η -parameters are fitted from the I -values given in [5] for the distances there; they are different for the first, second and third neighbour shell. For Fe, the situation is somewhat more complicated: There, the η -values for the three neighbour shells in fcc Fe are obtained from those contained in the results for bcc Fe in [5] with the interpolation procedure given in the appendix of [12].

This determines finally the paramagnetic part of our Hamiltonian: For the magnetic properties, in which we are finally interested, and also for the charge distribution in the magnetic state, self-consistency is then demanded, expressed by the terms proportional to $U_{l,\alpha}$ in eqn. (1). It is important that this self-consistency does not refer only to global properties, but actually it refers to the local values of all charge- and spin densities.

At the end, we comment on the parameter Δ_l in eqn. (1): If we want to generate a globally ferromagnetic state, we start everywhere with positive values $\Delta_l = 1$ eV, which are then switched off after the first iteration. In contrast, for the generation of spin glass states we use a more complicated procedure: At first, we start with a Δ_l , which is $\neq 0$ only for one Fe site (for which we usually take one surrounded by a large number of Ni atoms, since there seems to be a rather strong and positive exchange interaction between Fe and Ni). Then, in five iterations of eqn. (1), a nontrivial spin configuration develops in the whole sample, which is already almost self-consistent concerning the final moment directions, but not concerning the amplitudes; i.e. the spin configuration obtained has different signs of the spin polarization at different atoms. This distribution of signs may look random: Actually, it is not, since it reflects correlations due to the interactions in the system. So we now continue in iteration number 6 with transient Δ_l values of magnitude 1 eV everywhere, but with different signs at different l , namely the signs of the local spin polarization determined in the first five iterations. For the following iterations, the Δ_l are then switched off

completely, and the equations are iterated to self-consistency, which can take 100 iterations or even more. In this way, our spin glass configurations are generated, which still have self-consistently determined magnetic short-range order.

3 Results

3.1 Magnetic configuration

In Fig. 1, we present the magnetic phase diagram as determined experimentally by [6, 8]. Here, for $0.04 \leq y \leq 0.14$, one observes re-entrant spin glass behaviour, i.e. a transition from paramagnetic via ferromagnetic to spin glass behaviour, if the temperature is decreased. However, already at this point one should note that there exists a particular region between the ferromagnetic and the spin-glass regions, where both states apparently co-exist as metastable states. In fact, in Fig. 2 we show the results of our numerical simulation with ferromagnetic preparation: Here, up to $y \approx 0.07$, a nice agreement between the experimentally determined average moment and our results is found, whereas for larger y our calculated behaviour apparently continues as before in the ferromagnetic state with gradually decreasing average, whereas experimentally, there is a more drastic decrease to the spin glass phase. However, since in our calculation we use periodic boundary conditions with a periodicity length of only three fcc lattice constants and in view of the other approximations of our method, this discrepancy is perhaps not astonishing. Namely, throughout the same concentration region, by the above-mentioned spin glass preparation, we can also get the already mentioned metastable spin glass states with essentially vanishing average moment. A typical plot of the moment distribution in such a spin glass state is presented in Fig. 3 for a disordered $\text{Fe}_{0.65}\text{Ni}_{0.35}$ system.

Comparing the energy of the ferromagnetic and the spin glass states, we find that our ferromagnetic states are somewhat more favourable by energies of ≈ 6 meV per atom. However, as mentioned above, the accuracy of our method is not reliable enough to make this a significant statement. In fact, experimentally, see Fig. 1, the spin glass state seems to have lower energy; but at least the energy difference, corresponding to $T \approx 60K$, is of the same order.

In Fig. 4, we present histograms for the magnetic moment distributions of Fe-, Ni-, and Mn-atoms for 11 different Mn concentrations y of the *ferromagnetic states* calculated by our method for $(\text{Fe}_{0.65}\text{Ni}_{0.35})_{1-y}\text{Mn}_y$. Fig. 5 exhibits the average moments versus concentration. Interestingly, the Ni moments have apparently always well defined moments around $0.5 \mu_B$, whereas the Fe moment distributions are rather broad, e.g. they are spread between ~ 0.5 and $\sim 2.5 \mu_B$, for $y = 0.04$. Of course, details of the Fe distribution depend on the Mn concentration y , e.g. for $y = 0$ only Fe moments above $1.5 \mu_B$ are observed, whereas for $y \approx 0.05$ also moments around $0.5 \mu_B$ appear, but generally, the y -dependence of the *Fe*-moment distributions does not look drastic.

With the Mn moments itself, this is different: Some of the Mn atoms are polarized parallel to the majority spin direction, but the majority of the Mn atoms seems to be polarized antiparallel, as one can see from Fig. 5. Moreover, the magnitude of the Mn moments can vary drastically from site to site, which is not astonishing, since this was already true for α -Mn, [2].

For the *spin glass configurations* it is characteristic, see Fig. 6, that the Ni moments are no longer spread around $0.5 \mu_B$, but around zero. Further, for $y = 0.2$ both the Fe and the Mn moments are almost homogeneously distributed between $\approx -2 \mu_B$ and $\approx +2 \mu_B$. (For $y = 0$, the Fe moments are distributed between -2.5 and $+2.5 \mu_B$.)

In Fig. 7-9 we compare our calculated distributions for the Fe moments with hyperfine field measurements obtained by Mössbauer spectroscopy experiments [13]. For $y=0$ and $y=0.039$ (Fig. 7 and 8) there is good agreement between the experimental hyperfine field distribution and the magnetic moment distribution in the ferromagnetic state. For higher Mn-concentrations, e.g. $y=0.102$, the spin glass state corresponds better to the experimental result (Fig. 9). For each of this three concentrations we assume the same conversion factor of $14.5 \text{ T per } \mu_B$.

According to [13] the oscillatory structure of the hyperfine field distribution is of no physical relevance, but is simply a consequence of the fit procedure used by the authors.

A natural question is, whether the magnetic moments depend on the number of neighbouring atoms of the same or different kind. Therefore, in Fig. 10, we present some kind of plot, which allows answers on this

question: E.g., from this figure it is obvious that high Fe moments are favoured by a high number of Ni neighbours, and disfavoured by a high number of Mn neighbours, whereas the Ni moments themselves are rather insensitive on the neighbourhood. However, the spread of the distributions in Fig. 10 around the average data points should be kept in mind, when stating these tendencies, which can of course be quantified only on average, see the open circles in Fig. 10. Finally, it should be noted again that the magnitude of the Mn moments range between 0 and $\approx 2 \mu_B$, with typical values around $1 \mu_B$. Fig.11 presents similar plots for the spin glass configurations, where the width of the distributions is impressive, and the tendencies concerning Ni neighbours in case of Fe atoms are similar.

We have tried similar plots as in Fig. 10 and Fig. 11 also for the 2nd- and 3rd-nearest neighbour shell, however with non-conclusive results. Therefore, those plots are omitted.

3.2 Simplified spin model

In the following we try to describe the results for the magnetic behaviour with a simple molecular-field type *ansatz*. For the determination of the magnetic moments μ_l^z at the different sites l of the sample we have tried the equation

$$\mu_l^z = \sum_{k=1}^{42} c_{A(l),A(k)} \cdot \mu_k^z \quad (4)$$

In eqn. (4), the sum is over the 42 neighbours of site l up to the third-nearest neighbour shell, and there are nine coefficients per shell, namely $c_{A(l),A(k)} \in \{c_{Fe,Fe}; c_{Fe,Ni}; c_{Fe,Mn}; \dots; c_{Mn,Fe}; c_{Mn,Ni}; c_{Mn,Mn}\}$, depending on the occupation of the sites l and k by the respective kind of atoms. Qualitatively, the terms $c_{A(l),A(k)} \cdot \mu_k$ can be understood as composed of a local susceptibility χ_l times a local effective field $h_{l,k} \propto \mu_k^z$. In fact, fitting the coefficients to our results for μ_l^z , which we obtained by our itinerant approach, with the ansatz of eqn. (4), we obtain the results presented in Fig. 12. Although these results depend on the Mn concentration y , and although the statistical error bars, which we have omitted to show, are rather large, namely typically ± 0.06 , some conclusions can be drawn from Fig. 12: In the ferromagnetic state, the magnetization of Fe atoms is strongly influenced by the Ni

neighbors in the first neighbour shell, and up to $y \approx 0.1$ also by those of the second neighbour shell. In fact, while $c_{Fe, Ni}$ is as large as 0.3 for $y=0$ and increases up to 0.4 for larger y , $c_{Fe, Fe}$ is only around 0.06 for $y=0$ and even as low as 0.025 for $y > 0.1$; however, it should of course be taken into account that $\mu_{Ni} \approx 0.5$, while μ_{Fe} can be three or five times as large, so Ni is dominating, but not strongly. Moreover, the coefficient $c_{Fe, Mn}$ is negative over a considerable y -range and particularly strong in the 2nd-neighbour shell for small y -values, similar as $c_{Mn, Mn}$, whereas $c_{Fe, Fe}$ is positive in the ferromagnetic state, as mentioned above, contrary to a formerly wide-spread assumption ([14]). Also interesting is the strong scatter of the coefficients for Mn, i.e. the third column. This might show that the Mn moments tend to get "frustrated", however a definite statement cannot be made in view of the small number of Mn atoms.

Most important, however, is the fact that for the spin glass states (for which we omit the corresponding plots [15]) the coefficients are different from those of the ferromagnetic case presented in Fig. 12: The main difference concerns $c_{Fe, Ni}$, which becomes as high as 2.3 for $y=0$, 1.5 for $y=0.1$ and 1.4 for $y = 0.2$. This is understandable, since in the spin glass state also μ_{Ni} decreases in magnitude from $\approx 0.5 \mu_B$ to much smaller values (see above); however due to the increase of $c_{Fe, Ni}$, the Ni moments remain important for the Fe moments. A second important difference between the ferromagnetic and the spin glass states is that $c_{Fe, Fe}$, which was positive for ferromagnetic preparation, is negative (≈ -0.1) for spin glass preparation. So the implicit assumption made with the above-mentioned *ansatz*, namely that the $c_{A(i), A(k)}$ coefficients should not depend on the global magnetic state, is obviously not true. This means, one should better stay with the itinerant description, realizing that here the spin configuration is not fixed by given interaction coefficients as in Heisenberg spin glasses: Instead, the effective interactions depend on the global itinerant state and are different for a ferromagnetic and an itinerant spin-glass configuration of the system. Thus the itinerant description is really necessary.

3.3 Electrical resistivity in the magnetic state

It is perhaps not widely known that in a disordered crystalline or amorphous metallic system not only single particle properties, as just

discussed, but even two-particle properties as the electrical resistivity can be calculated by our semi-empirical LCAO formalism, namely by means of the Kubo formalism, [16]. In fact, in [16], the Kubo formalism has been successfully applied for the numerical calculation of the resistivity in the magnetic state of amorphous Fe/Zr alloys, and there we have also described how the conductivity $\sigma_{x,x}$ at T=0 K as a function of the Fermi-energy E_f can be calculated from the formula

$$\sigma_{x,x}(E_f) = \frac{e^2 \hbar \eta}{\Omega \Delta E} \sum_{\epsilon^{(\nu)} \in \Delta E} \langle v_x \vec{c}^{(\nu)} | [(E_f - H)^2 + \eta^2]^{-1} v_x \vec{c}^{(\nu)} \rangle. \quad (5)$$

Here the sum is over all ν with $\epsilon^{(\nu)} \in \Delta E$; further, Ω is the volume per atom, $\vec{c}^{(\nu)}$ an eigenstate of eqn. (1) with energy $\epsilon^{(\nu)}$ in the interval ΔE around E_f , and η is an effective line broadening parameter, which should be of the order of 1/2 the typical energy distance between neighbouring eigenvalues. Of course, the results depend on the choice of ΔE and of η , and additionally one has to perform sample averages and averages over the directions x , y , and z of the conductivity. Then, as we see in the Fig. 13 below, and as we have already found in [16], the result is essentially independent on ΔE and η :

In Fig. 13, we compare our results with the experiments in [10] and find good agreement, concerning the dependence on the Mn concentration y , to the accuracy considered, over the whole parameter range. However, there is one discrepancy, which we do not yet understand at present, namely our resistivities are always too large by a factor ≈ 5 , compared with the experiment. But in view of the approximations involved in the evaluation of eq. (5) and in view of the large scale of resistivities of different metals this discrepancy should perhaps not be taken too serious. In fact with $\eta \approx 0.02$ eV we induce effectively inelastic scattering events corresponding to T ≈ 200 K, and the effect of $\Delta E \approx 0.2$ eV may even be larger, whereas the experimental values in our comparison are at 4 K. However, at 300 K, according to [10], the experimental values would only be enhanced with respect to those at 4 K by factors between 1.8 (for $y=0$) and 1.1 for $y = 0.084$. Additionally, the conductivity should be influenced by transverse components of magnetic moments, which we have neglected.

4 Discussion

We have studied the magnetic behaviour of Fe-Ni-Mn alloys in the sensitive regime around the Fe-Ni Invar-region, [3], i.e. $(\text{Fe}_{0.65}\text{Ni}_{0.35})_{1-y}\text{Mn}_y$, where with increasing Mn concentration y a transition from ferromagnetic to spin glass behaviour has been observed experimentally, [6, 8].

Actually, with our semi-empirical LCAO approach we have found that both ferromagnetic states and also itinerant spin glass states can be prepared and are metastable in the whole concentration region considered. These different states have roughly the same energy, i.e. according to our calculation, the ferromagnetic state appears to be slightly favoured by ~ 6 meV per atom; however our method is not accurate enough for a definite statement. In any case this implies that the itinerant magnetism of these alloys is quite complicated and cannot simply be described by the Heisenberg model, since one has e.g. a broad distribution of different values of the magnitudes of the local atomic moments, both for Fe and Mn.

Starting our iterations with a homogeneous ferromagnetic state, we obtained good agreement with experimental results in the ferromagnetic state up to a Mn concentration of $y \approx 0.07$. For higher concentrations, more realistic results (e.g. the already mentioned spin-glass states with vanishing total magnetic moment, but non-trivial local moments) have been obtained systematically from a self-consistently prepared inhomogeneous state with correct short range magnetic order. Thus there seems to be some kind of preparation dependence of the equilibrium state. After all, this is typical for a situation with possible spin-glass behaviour and not in contradiction to the experimental situation, see [6].

Finally, we have also calculated the electrical resistivity in the magnetic state in our LCAO formalism by an implementation of the Kubo formalism (see [16]), and we obtained good agreement with experiments apart from the fact that our conductivities are generally too low by a factor of ≈ 5 , compared with experiments. The problem, whether the conductivity in the magnetic state will change with the introduction of transverse spin components, remains to be studied in the future.

Acknowledgements

Two of the authors (U. K. and F. S.) would like to thank the Institute of Molecular Physics of the Polish Academy of Sciences in Poznań for its hospitality and particularly Dr. S. Krompiewski and Prof. J. Morkowski for useful discussions.

References

- [1] H. Früchtl and U. Krey, *J. Magn. Magn. Mater.* **94** (1991) L20.
- [2] J. Süß and U. Krey, *J. Magn. Magn. Mater.* **125** (1993) 351.
- [3] E. F. Wassermann, *INVAR: Moment-Volume Instabilities in Transition Metals and Alloys*, in: *Ferromagnetic Materials*, vol. 5, ed. K. H. J. Buschow (North Holland, Amsterdam, 1990).
- [4] U. Krauss and U. Krey, *J. Magn. Magn. Mater.* **98** (1991) L1.
- [5] D. A. Papaconstantopoulos, *Handbook of the bandstructure of elemental solids* (Plenum Press, New York 1986).
- [6] C. Böttger, *Der Magnetismus des Systems $(Fe_{0.65}Ni_{0.35})_{1-x}Mn_x$* , Dissertation, TU Braunschweig, 1992 (in German).
- [7] C. Böttger, H. Friedrichs, H. Neuhäuser and J. Hesse, *Physica B* **161** (1989) 29.
- [8] J. Hesse, C. Böttger, A. Wulfes, J. Sievert and H. Ahlers, *Phys. status sol. (a)* **135** (1993) 343.
- [9] M. Fricke and J. Hesse, *Hyperfine Interactions* **70** (1992) 1105.
- [10] C. Böttger, J. Hesse, *Z. Physik B* **75** (1989) 485
- [11] W.A. Harrison, *Electronic Structure and the properties of solids*, (Freeman, San Francisco 1980)
- [12] S. Krompiewski, U. Krey and H. Ostermeier, *J. Magn. Magn. Mater.* **69** (1987) 117.
- [13] B. Huck and J. Hesse, *J. Magn. Magn. Mater.* **78** (1989) 247-254 .

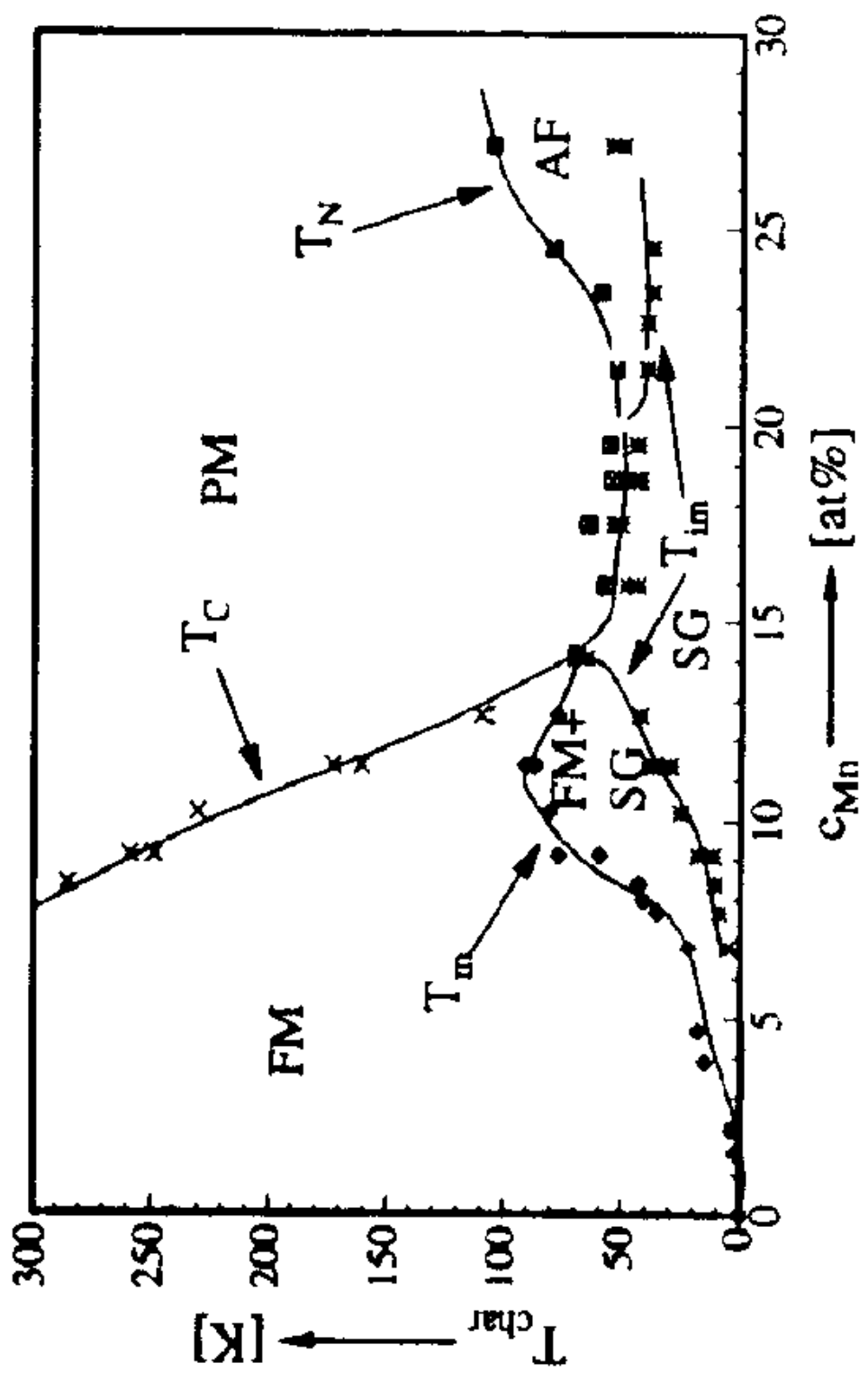
- [14] R. Kloss, Intern. J. Magn. 5 (1973) 251.
- [15] A. Paintner, Diploma thesis, Univ. Regensburg 1994 (unpublished)
- [16] U. Krey, U. Krauss, S. Krompiewski, T. Stobiecki, J. Magn. Magn. Mater. 116 (1992) L7.

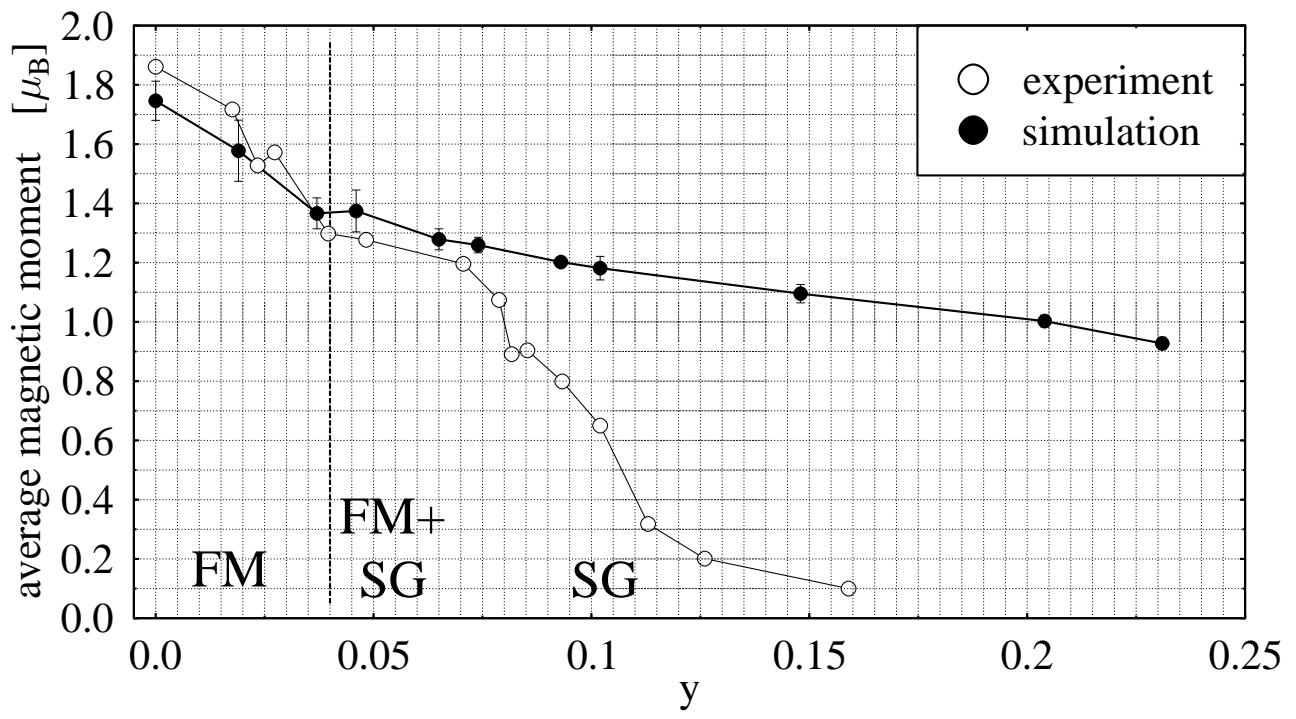
Figure Captions

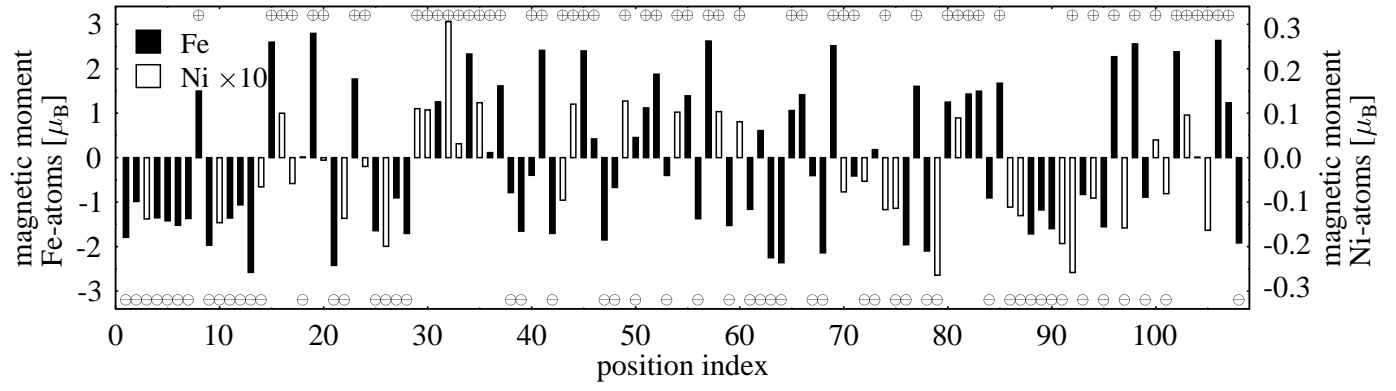
- Fig. 1: Magnetic phase diagram for the system $(Fe_{0.65}Ni_{0.35})_{1-y}Mn_y$, from [6,8].
- Fig. 2: Magnetization of the alloy system $(Fe_{0.65}Ni_{0.35})_{1-y}Mn_y$ versus Mn-concentration y .
- Fig. 3: Typical moment distribution of a spin glass state for a disordered $Fe_{0.65}Ni_{0.35}$ alloy. The Ni moments are scaled by a factor 10. The symbols \oplus above and \ominus below an atomic position show the local spin direction of the atoms at the intermediary state in the 6-th iteration (see text).
- Fig. 4: Calculated histograms for the magnetic moment distribution of Fe-, Ni- and Mn-atoms for Mn concentrations y in the range $0 < y < 0.231$ (ferromagnetic preparation).
- Fig. 5: Average magnetic moments for the three different alloy components Fe, Ni and Mn.
- Fig. 6: Calculated histograms for the magnetic moment distribution of Fe-, Ni- and Mn-atoms for Mn concentration $y \in \{0; 0.102; 0.204\}$ (spin glass preparation).
- Fig. 7: Calculated magnetic-moment probability histogram and measured hyperfine field probability distribution (dashed-line fit) of the system $Fe_{0.65}Ni_{0.35}$. The simulation was done with ferromagnetic preparation. A conversion factor of $H = 14.5 T$ per μ_B is assumed.
- Fig. 8: Calculated magnetic-moment probability histogram (ferromagnetic preparation) of the system $(Fe_{0.65}Ni_{0.35})_{0.963}Mn_{0.037}$ and measured hyperfine field probability distribution (dashed-line fit) of the system $(Fe_{0.65}Ni_{0.35})_{0.961}Mn_{0.039}$.
- Fig. 9: Calculated magnetic-moment probability histogram (spin glass preparation) of the system $(Fe_{0.65}Ni_{0.35})_{0.898}Mn_{0.102}$ and measured hyperfine field probability distribution (dashed-line fit) of the system $(Fe_{0.65}Ni_{0.35})_{0.919}Mn_{0.084}$.
- Fig. 10: Influence of the local neighbourhood on the magnitude of the magnetic moments for final states with ferromagnetic preparation. In the left three columns the magnitude of the Fe moments is plotted versus the next neighbour number of Fe-, Ni- and Mn-neighbours for six different Mn concentrations. In the middle three columns the same is plotted for Ni, and in the right three columns for Mn. The dashes represent the single values and the circles are the averaged values.
- Fig. 11: Influence of the local neighbourhood on the magnitude of the magnetic moments for final states with spin glass preparation.

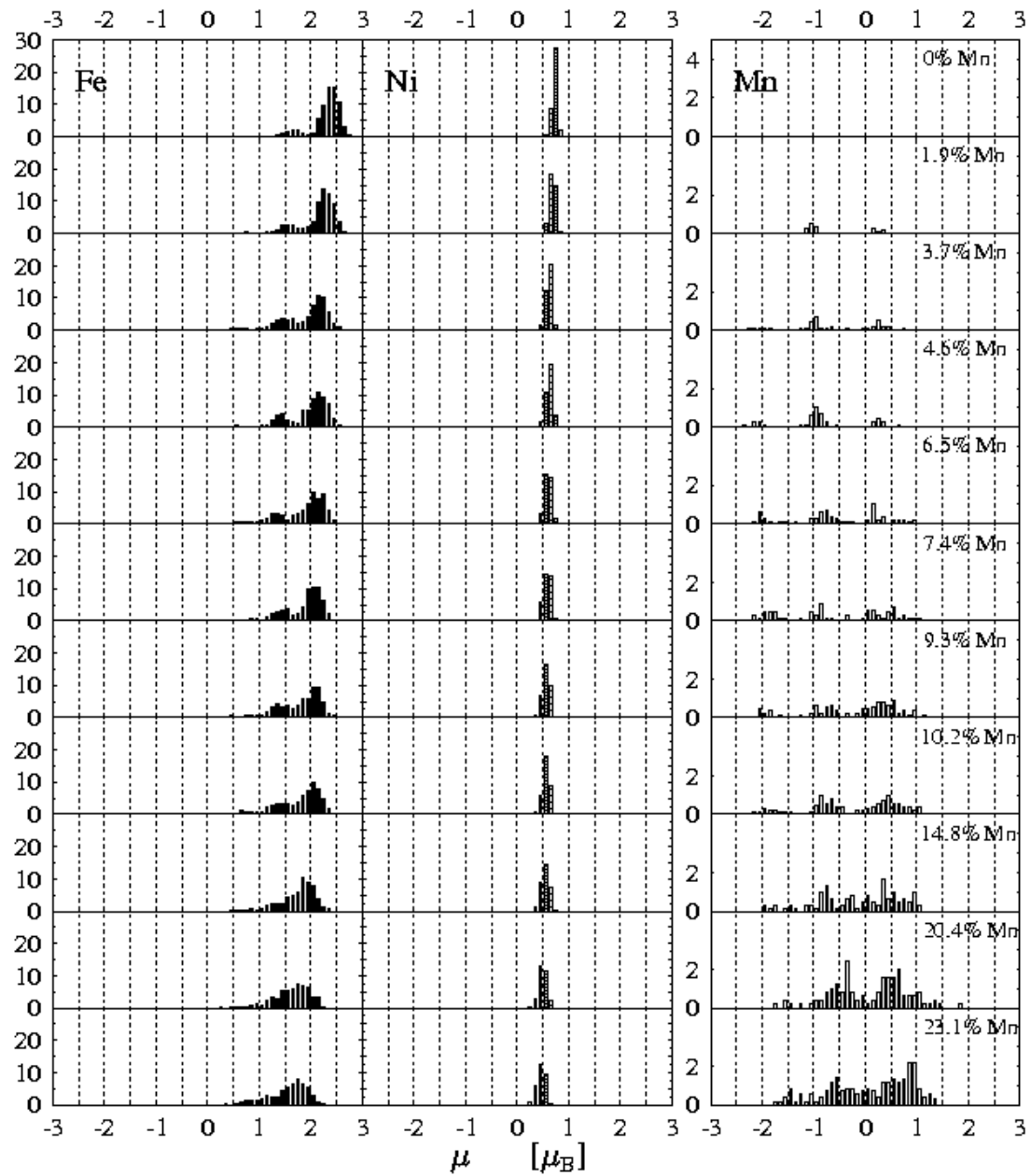
Fig. 12: The coefficients $c_{A(l),A(k)}$ from equation (4) are plotted against Mn concentration y for states with ferromagnetic preparation. The coefficients of the first row are related to next neighbours. Those of the second and third row are related to second resp. third neighbour shells.

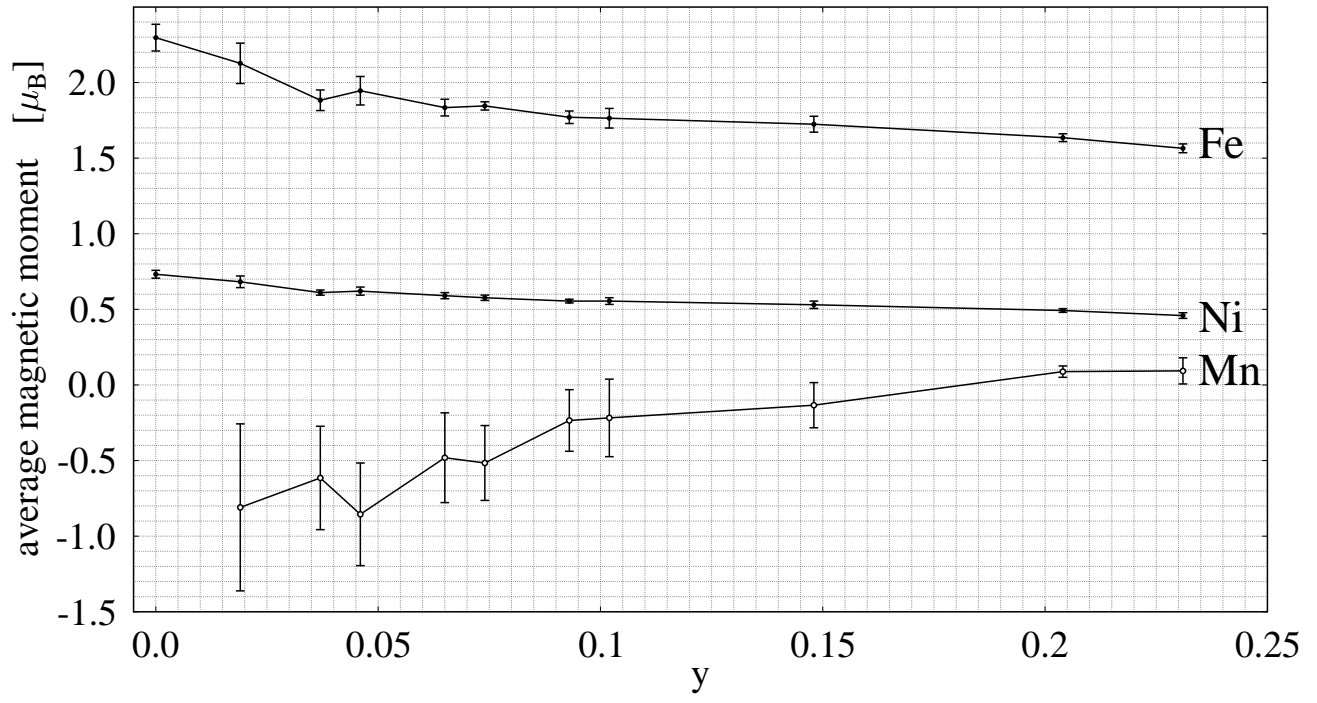
Fig. 13: Measured and calculated conductivities against Mn concentration for several combinations of the parameters η and ΔE .

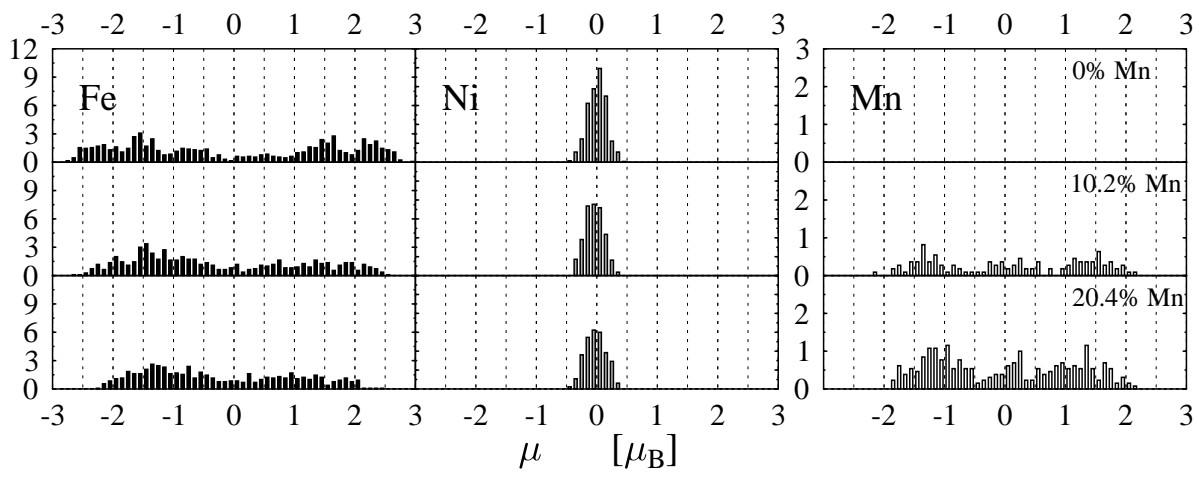


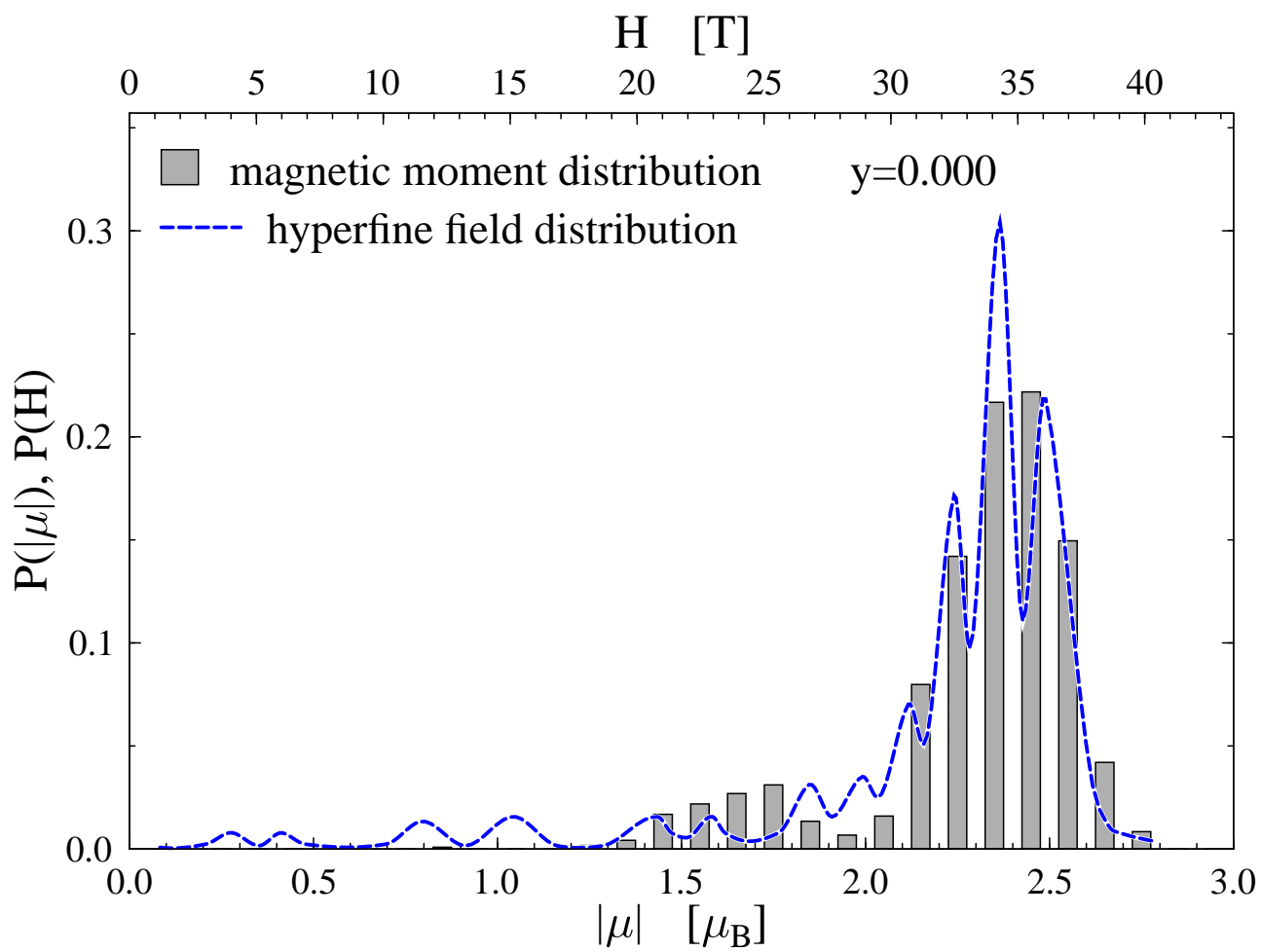


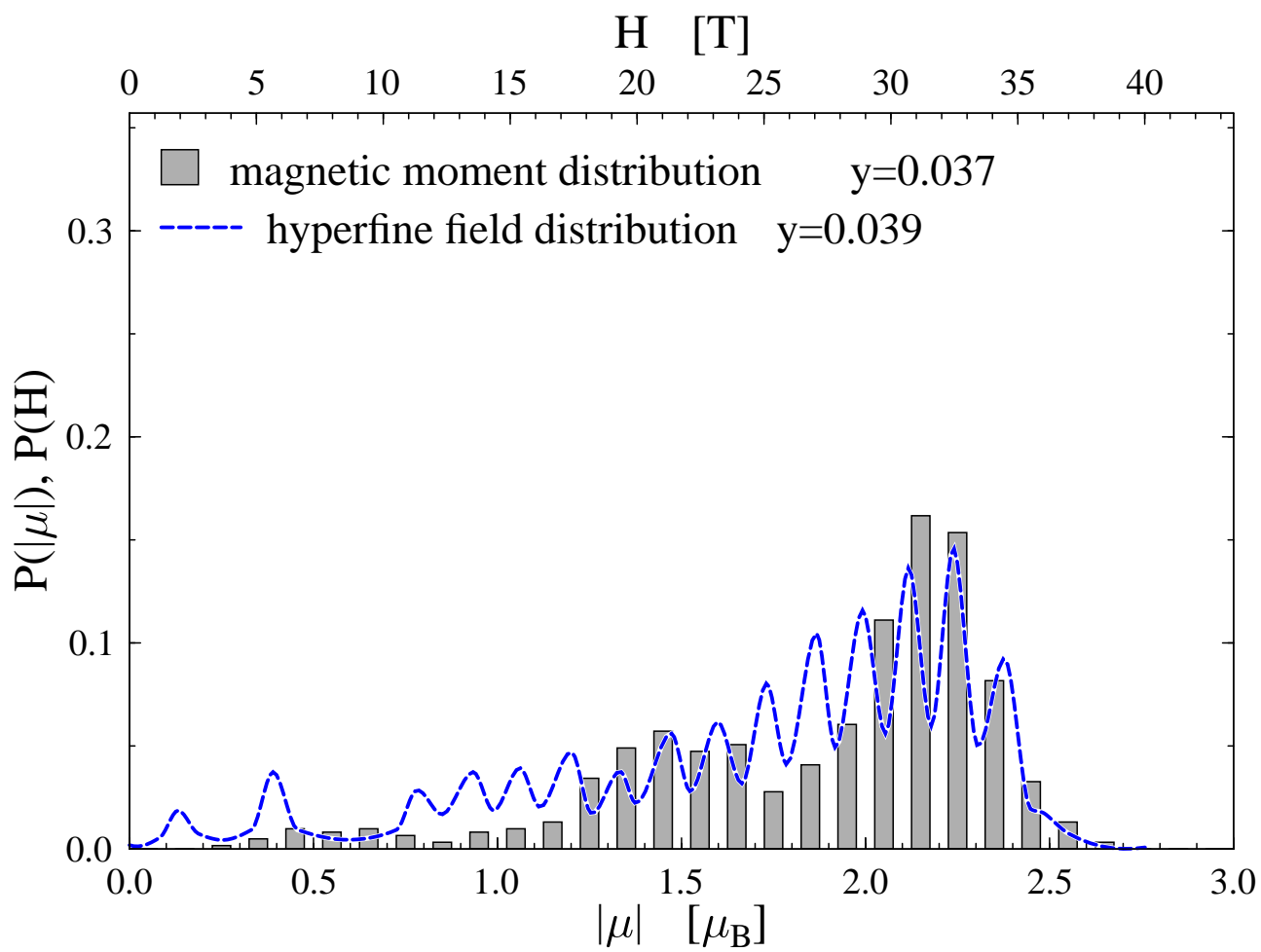


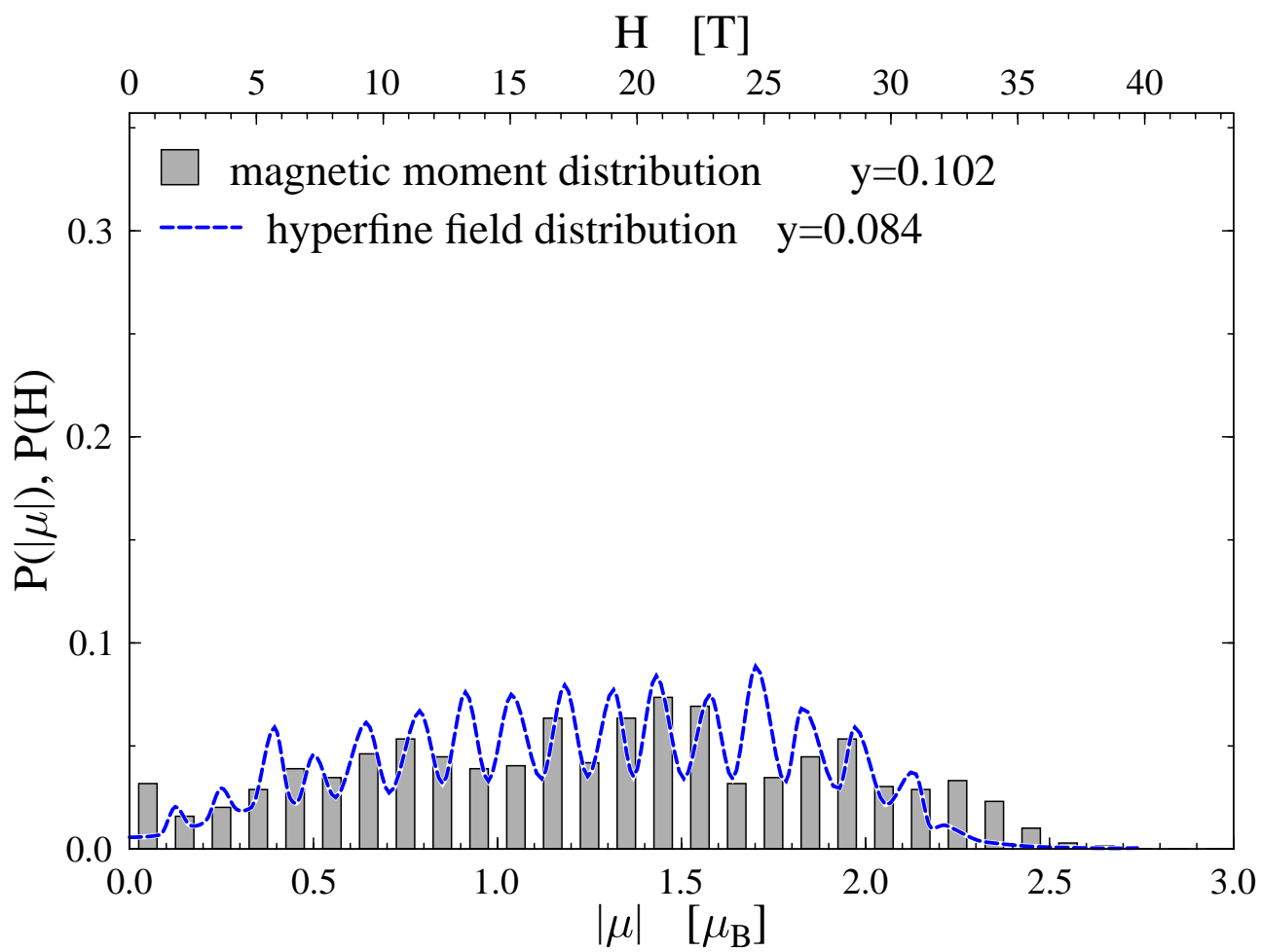




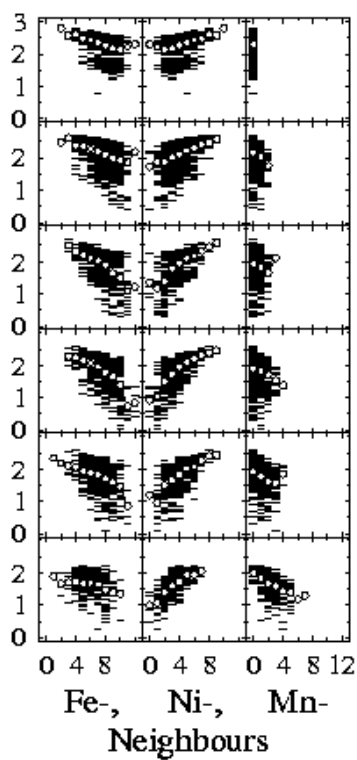




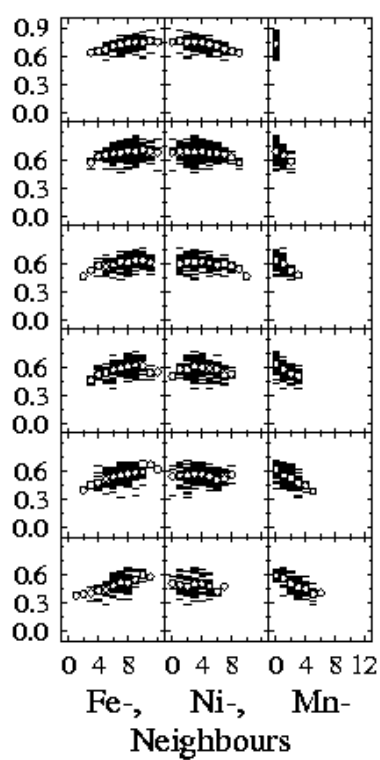




Fe



Ni



Mn

